Polar Science 16 (2018) 1–9

Contents lists available at ScienceDirect

Polar Science

journal homepage: www.elsevier.com/locate/polar

Arctic-midlatitude weather linkages in North America

James E. Overland[a,*], Muyin Wang[a,b]

[a] NOAA/Pacific Marine Environmental Laboratory, Seattle WA, USA
[b] University of Washington/JISAO, Seattle WA, USA

ARTICLE INFO

Keywords:
Arctic
Jet stream
Sea ice
Weather linkages
North America

ABSTRACT

There is intense public interest in whether major Arctic changes can and will impact midlatitude weather such as cold air outbreaks on the central and east side of continents. Although there is progress in linkage research for eastern Asia, a clear gap is conformation for North America. We show two stationary temperature/geopotential height patterns where warmer Arctic temperatures have reinforced existing tropospheric jet stream wave amplitudes over North America: a Greenland/Baffin Block pattern during December 2010 and an Alaska Ridge pattern during December 2017. Even with continuing Arctic warming over the past decade, other recent eastern US winter months were less susceptible for an Arctic linkage: the jet stream was represented by either zonal flow, progressive weather systems, or unfavorable phasing of the long wave pattern. The present analysis lays the scientific controversy over the validity of linkages to the inherent intermittency of jet stream dynamics, which provides only an occasional bridge between Arctic thermodynamic forcing and extended midlatitude weather events.

1. Introduction

Assessment of the potential for recent Arctic changes to influence broader hemispheric weather continues to be controversial (NRC, 2014; Overland et al., 2016; Francis et al., 2017; Kretschmer et al., 2018). Despite numerous workshops and a growing literature, convergence of understanding is lacking, with major objections about possible large impacts within the scientific community (Wallace et al., 2014). There is little agreement on problem formulation, analysis methods, diverse mechanisms, or public statements from the research community. The topic, however, is meteorologically consequential and a major science challenge, as Arctic changes are an inevitable aspect of continued anthropogenic global warming, and Arctic weather linkages are a potential opportunity for improved extended-range forecasts at midlatitudes (Jung et al., 2015).

The important aspect of present Arctic weather linkages research is thus the failure to achieve consensus. Consensus is an overwhelming agreement among scientists and achieved through replication, the publication process, communication at conferences, and peer review. Kuhn (2012) noted that during periods of new scientific uncertainty that one should expect diversity, disagreements, and fragmentation of the scientific community. A recent review laid part of the controversy on shortcomings in experimental design and metrics used in some studies (Francis, 2017). The present paper hypothesizes that part of the controversy stems from internal variability in jet stream dynamics. The jet stream is a major intermediary between thermodynamic forcing in the Arctic of atmospheric circulation through the thermal wind relationship and resulting midlatitude weather elements (Cohen et al., 2014; Overland et al., 2015). We review potential North American (NA) case studies during the previous decade as a way forward to understand the role of intermittency and state dependence in Arctic/midlatitude linkages.

2. The temperature/geopotential height relationship

Whether thermodynamic changes (surface energy fluxes from warm SST anomalies and sea-ice loss, or temperature gradients) can be connected to atmospheric dynamics and wind systems, is given by the thermal wind equation and geopotential tendency equation (Holton, 1979; Overland and Wang, 2017); the latter is expressed in words as:

Geopotential Height Change (*is proportional to*) (Vorticity Advection) + decrease with height of [(*Temperature Advection*) + (*Thermal Heating*)] (1)

Geopotential heights can change, and thus modify wind fields, by (first term) horizontal propagation of existing jet stream features that can be considered primarily a chaotic part of atmospheric dynamics, (second term) bringing low-level warm, less dense air into a region, or (third term) warming a region locally at low levels. Part of the difficulty with linkage research is determining the influence of the third term,

* Corresponding author. NOAA/PMEL, 7600 Sand Point Way NE, Seattle, WA 98115, USA.
E-mail address: james.e.overland@noaa.gov (J.E. Overland).

https://doi.org/10.1016/j.polar.2018.02.001
Received 16 October 2017; Received in revised form 12 January 2018; Accepted 7 February 2018
Available online 10 February 2018

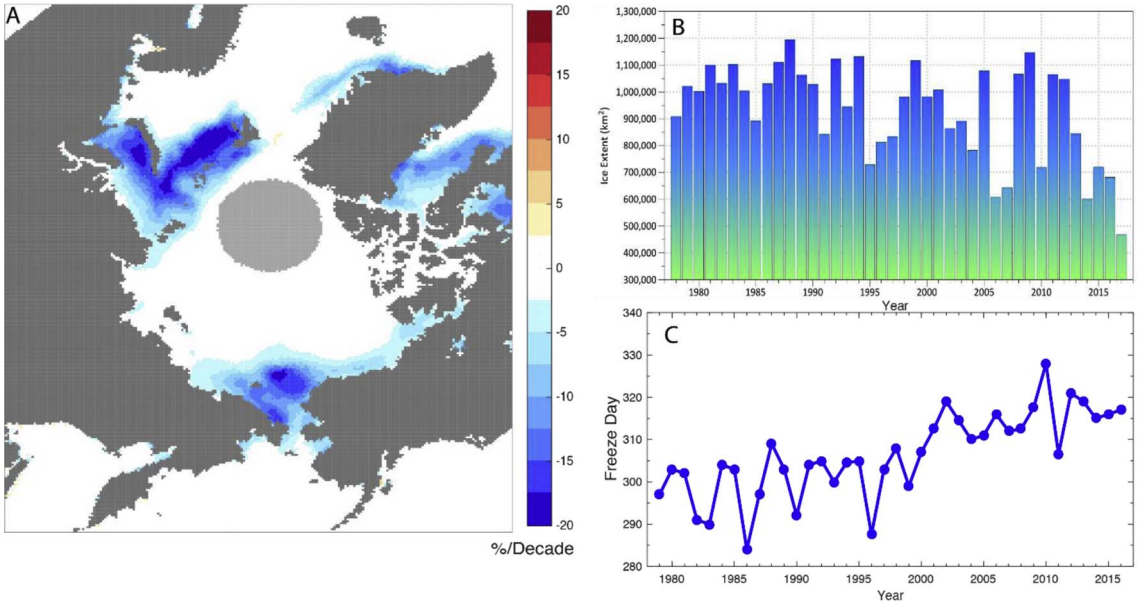

Fig. 1. A) Spatial map of the linear trend of sea ice concentration for November, the nominal time of autumn sea ice freeze-up, that implies a 40% loss in the Chukchi Sea and Baffin Bay over the satellite observation period 1979–2016). Units are percent per decade. Data are obtained from NSIDC. B) Chukchi Sea sea ice cover index for late November based on NSIDC passive microwave data (From Thoman personal communication). C) Freeze up dates for Baffin Bay (From Ballinger et al., 2017).

Arctic sources, relative to advective contributions to geopotential height changes. In particular we should look for linkage cases where the geopotential height fields are mostly stationary (lasting a week or more) so that the first vorticity advection term would be relatively small.

3. North American case studies from the previous decade

3.1. Sea ice changes

Historical decrease of Arctic-wide sea ice extent at the end of the summer season show a dramatic reduction beginning in 2007 to at or below −19% relative to the 1981–2010 mean (NSIDC, https://nsidc.org/data/seaice_index/compare_trends). Before then it is less clear whether forcing of Arctic/midlatitude weather linkages are large enough to be unequivocally detected.

Another important result is that potential linkages are regional (Overland et al., 2015). For example Fig. 1A shows the spatial pattern of the 1979–2016 trend in sea ice concentration for late freeze-up in November; units are percent per decade. Two NA regions stand out, the Chukchi Sea and Baffin Bay/northern Hudson Bay with concentration reductions of over 40% over the period of record. Fig. 1B shows the Chukchi Sea sea ice extent time series for the end of November; many but not all years since 2005 have lower values than years before 1995. 2017 was the record low autumn sea ice year for the Chukchi Sea (based on December 1st sea ice concentration). Baffin Bay had late freeze up (Fig. 1C) in all recent years since 2001 except for 2011 Note the low Chukchi sea ice and late Baffin freeze-up date in 2010. The last decade for these two regions has the potential for increased heat transfer to the lower atmosphere in late fall/early winter. However, there remains difficulties in detecting a sea ice loss signal in a noisy atmospheric response.

3.2. Previous studies for NA

We begin by assessing teleconnection patterns between eastern US cold events and high latitude atmospheric temperature and geopotential height fields beginning in 1950, regardless of potential sea ice forcing. Konrad (1996, his Fig. 3c), Messori et al. (2016, their Fig. 1h) and Xie et al. (2017, their Fig. 5c) show NA geopotential height field teleconnections during composite major eastern US winter cold events. All these figures show higher geopotential heights both over Alaska continuing along the western coast of NA, and west of Greenland. In investigating individual winters, positive height anomalies in these two northern regions can individually co-occur with cold US east coast events, or both can occur simultaneously. We label them as the Alaskan Ridge (AR) pattern and the Greenland-Baffin Bay Blocking (GBB) pattern.

With respect to AR based on models, Mills et al. (2016) note that Alaskan marine Arctic sensible heat flux anomalies during autumn can build planetary wave patterns that propagate downstream into NA midlatitudes, creating robust surface cold anomalies in the eastern US. Kug et al. (2015) show negative correlations between positive Alaskan marine Arctic surface air temperature anomalies with eastern US cold temperatures and geopotential height fields during December–February for the period 1979/1980–2013/2014 from reanalysis data. Lee et al. (2015) notes sea ice and North Pacific contributions for a cold eastern US 2013–2014 event. From inspection of the time series of Alaskan Arctic winter temperatures in these papers, it is evident that rather than showing a monotonic trend with time, there are event-like extreme cases such as winters of 2010–11 and 2013–14.

With respect to the GBB region, Ballinger et al. (2017) report that Greenland Blocking patterns [high geopotential height anomalies] and the incidence of meridional wind circulation patterns have increased over the modern sea ice decrease monitoring era, 1979–2014. They attribute this connection to ocean–atmosphere sensible heat exchange through ice-free or thin ice-covered seas. Temperature composites for years of extreme late freeze conditions, occurring since 2006 in Baffin Bay, reveal positive monthly surface air temperature departures that often exceed +1 standard deviation. Freeze onset dates were particularly late in 2010 and 2012 (Ballinger et al., 2017, their Fig. 2 and our Fig. 1C). Chen and Luo (2017) found that the frequency of Greenland Blocking events is significantly increased in the last decade because of intensified Arctic warming related to the large sea ice decline over the Baffin Bay, Davis Strait, and Labrador Sea; an associated intense cold anomaly is seen over the eastern North America.

Other authors note that cold eastern US temperatures are associated with the phasing of Northern Hemispheric-wide patterns, a wave number 5 circum-global pattern (Harnik et al., 2016) or a Tropical/Northern Hemisphere pattern (Ogi et al., 2016). With regard to

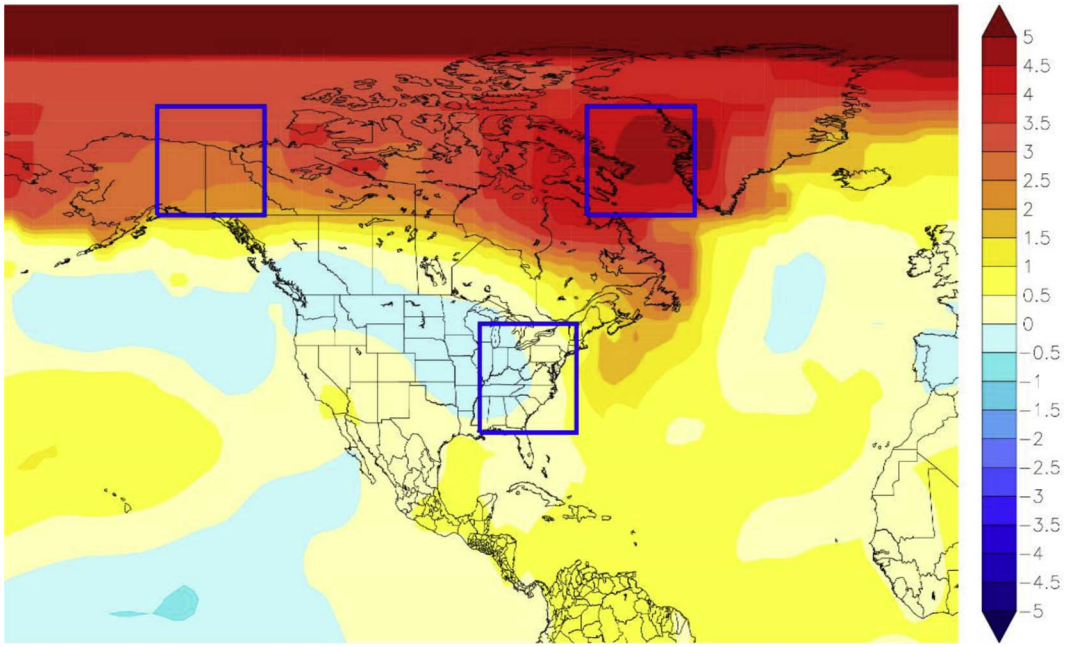

Fig. 2. Winter surface air temperature trends for 1990–2017 (based on NASA data https://data.giss.nasa.gov/gistemp and similar to Cohen et al. (2014)). Blue box over eastern North America outlines the domain used to compute monthly temperature anomalies. Boxes over Alaska and to the east of Greenland are the domain for calculating monthly geopotential height anomalies to assign Alaska Ridge (AR) and Greenland/Baffin Blocking (GBB) cases in Table 1. (For interpretation of the references to colour in this figure legend, the reader is referred to the Web version of this article.)

potential linkages, importantly, the AR pattern is located such that delayed sea ice formation in the Chukchi and Beaufort Seas could reinforce an AR geopotential height field through increased geopotential thickness (Fig. 1A and Eqn. (1)). Likewise Baffin and Hudson Bay are located so that delayed sea ice formation can reinforce the GBB.

3.3. Cold winters in eastern North America

The locations of late fall freeze-up in Fig. 1A and the correlation studies of AR (Kug et al., 2015) and GBB (Ballinger et al., 2017) are intriguing for the NA linkage question. A way forward is beginning with a quantitative consideration of historical cold cases in eastern NA and associated large scale geopotential height field patterns. We select a region for the eastern US to study cold events that is bounded by 30–45° N and 90 to 72° W as shown in Fig. 2. To exclude ocean areas a land-sea mask is applied to the temperature anomaly field. The limits of this domain are motivated by previous studies of eastern NA cold events (Grotjahn et al., 2016; Singh et al., 2016; Messori et al., 2016). Monthly areal average 2 m air temperature anomalies (T_{2m}) were computed for this region from the NCEP/NCAR reanalysis beginning in 1950. As a criterion for a cold event, we selected early winter months when the areal mean temperature anomaly was equal to or below one standard deviation for each month, listed for December and January in Table 1. Twenty cold-month events are found; only four occurred after 2007, in winters 2010–11 (December and January), 2014 (January), and 2017 (December).

Fig. 3A shows the composite pattern of near surface 925 hPa air temperatures that occurs during the combined 20 eastern NA monthly December and January cold events. Fig. 3B illustrates the associated 700 hPa geopotential height composite anomaly fields for these cold eastern NA events. The two large positive geopotential height anomaly regions (AR and GBB) are nearly collocated with the two positive low level temperature anomaly regions, supporting a surface temperature anomaly/atmospheric geopotential thickness connection. Positive

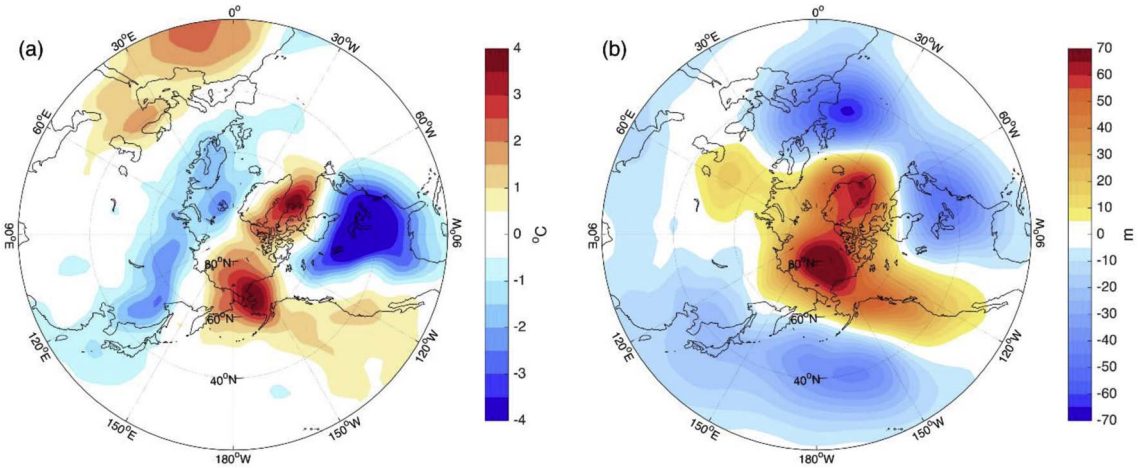

Fig. 3. A) Composite near surface (925 hPa) temperature anomaly field and B) 700 hPa geopotential height field for 20 cold eastern North American winter months from Table 1. Data from NCEP-NCAR reanalysis..

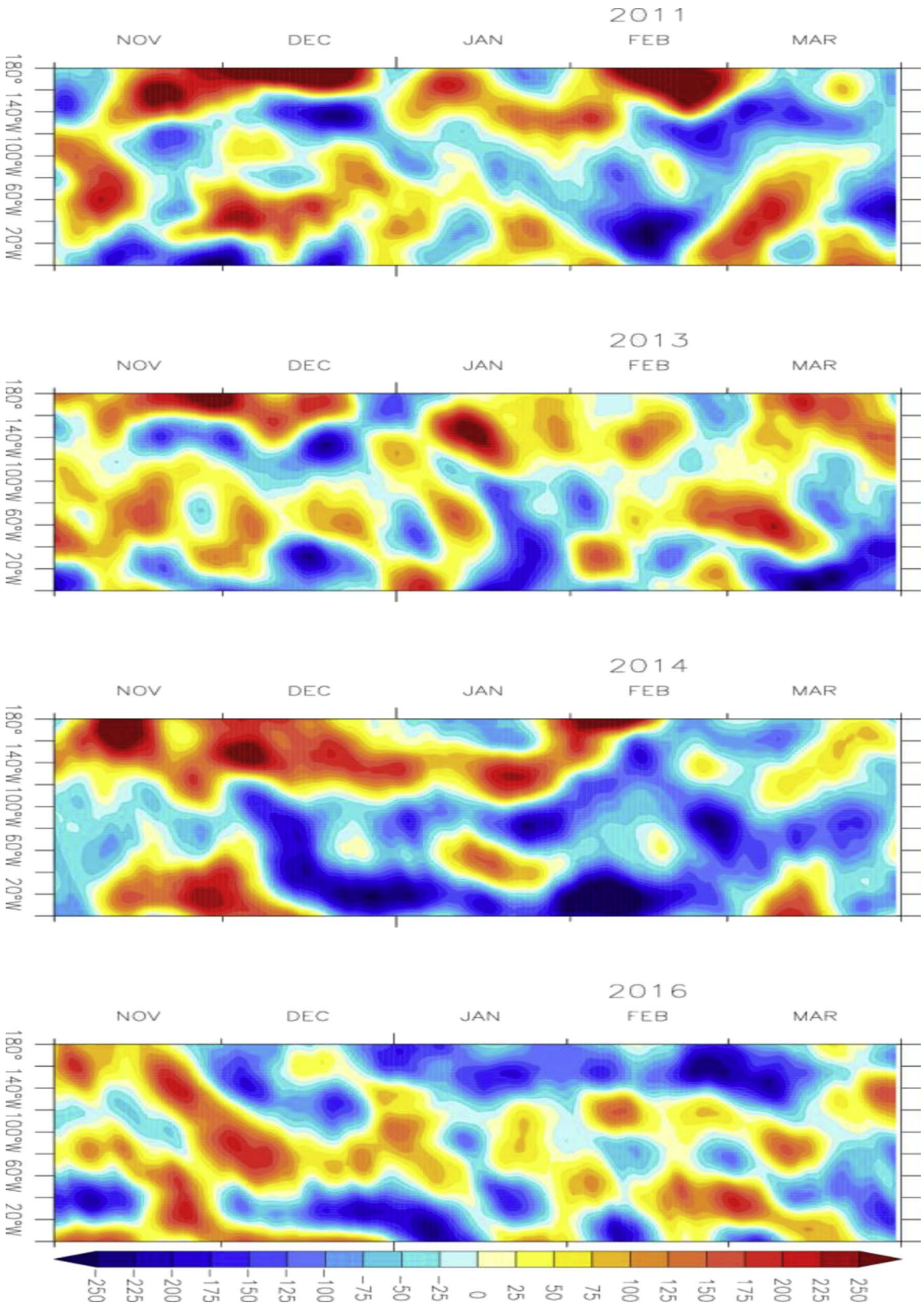

Fig. 4. From top down: A, B, C. D. Hovmoller plots of longitude-time section of 500 hPa geopotential height anomalies along 52° N for the period of Nov. 1 to the following year of March 31. Panels for 2010/11 and 2013/14 are for GBB and AR winters, and winters of 2012/13, 2015/16 show more progressive eastward movement of features. Data is from NCEP. NCAR daily Reanalysis and a 10-day running mean is applied.

temperature and geopotential height anomaly maximums in individual months can occur either near Alaska, near west Greenland, or in combination. To quantify the strength of AR and GBB patterns, AR and GBB index are constructed from 700hPa geopotential height anomalies averaged over two boxes, (AR box 60-75° N, 150-130° W and GBB box 60-75° N, 70-50° W) shown in Fig. 2, and their monthly values are listed in Table 1. All 20 cases were then separated by their maximum height anomaly values (Table 1) into Alaskan Ridge (AR), Greenland Baffin

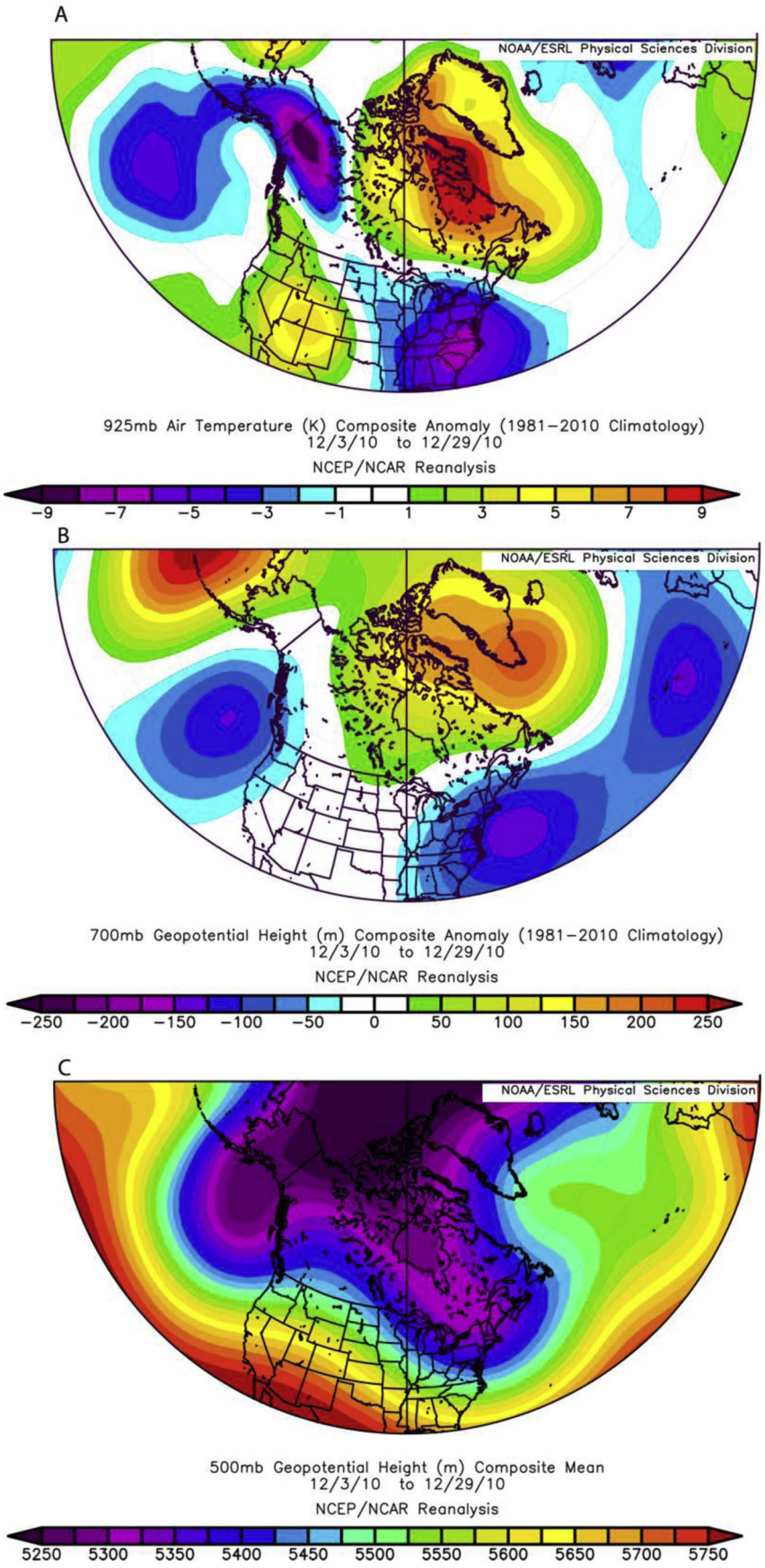

Fig. 5. Fields that represent a Greenland Baffin Blocking case from December 2010. A) 925 hPa air temperature anomaly, B) 700 hPa geopotential height anomaly, C) 500 hPa height field. Figures derived from the NOAA ESRL plotting routines.

Table 1
List of cold winter months for the eastern US (see Fig. 2) from 1950 through 2017. Case criteria is a value of less than 1 standard deviation in the temperature anomaly. Column 2 and 3 are the values of the geopotential height anomaly for the AR and GBB regions as shown in Fig. 2.

December	GBB-index	AR-index	Pattern Assigned	January	GBB-index	AR-index	Pattern Assigned
1958	34	53	Both	1963	95	98	Both
1960	−36	52	AR	1966	142	30	GBB
1963	11	57	AR	1970	63	29	Both
1976	21	−3	GBB	1977	121	65	GBB
1983	−29	110	AR	1978	−19	86	AR
1985	48	69	Both	1985	86	75	Both
1989	−5	53	AR	1994	7	74	AR
2000	86	73	Both	2003	42	54	Both
2010	177	2	GBB	2011	111	46	GBB
2017	22.6	80.	AR	2014	10	42	AR

Table 2
Eastern US (30–45°N, and 90-78°W) T2m temperature anomaly (1981–2010 climatology) for the given month based on NCEP/NCAR Reanalysis.

Year	December	January	Year
2006	2.9	1.9	2007
2007	1.7	−0.1	2008
2008	0.5	−1.9	2009
2009	−0.6	−2.5	2010
2010	−4.1	−2.6	2011
2011	2.4	2.2	2012
2012	2.9	1.7	2013
2013	0.8	−3.1	2014
2014	2	−1	2015
2015	6.7	−0.6	2016
2016	0.9	3.1	2017
2017	−0.9		2018

Block (GBB), or Both cases.

December and January eastern NA cold temperature years after 2007 (Table 2) show one strong GBB (December 2010) and three AR (strong: December 2017, and weak: January 2011 and January 2014) cold cases, with stationary height field patterns as discussed in the follow sections. Other recent years with warmer eastern NA winters do not have high amplitude north—south oriented height fields where late freeze up in the Chukchi Sea or Baffin/Hudson Bay could support a high amplitude height pattern. Examples of these alternate large scale atmospheric height fields (zonal, progressive, and unfavorable phasing) are further addressed in section 3.6.

3.4. 2010–11, a strong GBB winter

Hovmoller plots provide a time/longitude history of propagation of geopotential height for various winters as a means to address a more granular level of detail than monthly averages. Fig. 4 shows a Hovmoller time/longitude plot for selected winters of 500 hPa geopotential height anomalies for the Western Hemisphere along 52° N for the period of Nov. 1 to the following year of March 31.

Fig. 4A for winter 2010–2011 show a stationary positive anomaly height feature along 45° W for December 2010 to early January 2011; this represents a persistent GBB event. Northern Baffin Bay showed large positive temperature anomalies at 925 hPa of greater than +10 °C beginning 20 November 2010. Weather systems over the US were rather progressive in November, but very cold conditions were established over the southeastern US by 3 December (Fig. 5A). By this time a warm temperature anomaly was centered over the southern Baffin Bay. This was the principal year that Ballinger et al. (2017) document a late freeze-up date (Fig. 1C). Positive geopotential height anomalies (Fig. 5B) coincided with the region of positive temperature anomalies (Fig. 5A), diverting the northwesterly flow from central Canada into Virginia and North Carolina (Fig. 5C). There was a weakening of the southeastern US event in 11–13 December, but a quick return to cold conditions. After a New Year's break, the GBB pattern returned from 6 to 14 January 2011 (Supplemental Fig. S1).

The cold eastern US temperatures in January 2010 was not selected as an extreme historical cold case, but it comes in just above the threshold (Table 2). Inspection of the January 2010 temperature and geopotential height fields (Supplemental Fig. S2) show that this month can be considered a possible weak GBB linkage case.

Some spatial shifts between the sea ice free area, low level temperatures, and geopotential anomalies are to be expected, as the geopotential height fields are impacted by advective components beyond surface forcing (Eqn. (1)).

3.5. 2017–18, a strong AR winter

December 2017 and extending into early January was a strong AR case, which corresponds to the lowest observed sea ice coverage in the Chukchi Sea for December 1 (Fig. 1B). At least 17 deaths in the eastern US were recorded (Associated Press, 4 January 2018) and extensive transportation disruptions, record cold temperatures, and power losses were experienced. Fig. 6A shows the 925 hPa air temperature anomaly field for 8 December 2017 through 7 January 2018. While the North America AR ridge/trough dipole feature was present during most of this monthly duration (Fig. 6B), the extreme amplitude of the AR pattern was particularly strong in the second half of December. This case matches the maximum Chukchi sea ice loss December and is a candidate for Arctic reinforcement of the AR pattern.

Despite considerable interest in winter 2013–14 in the literature corresponding to drought in California (Liu et al., 2015; Baxter and Nigam, 2015; Singh et al., 2016), most weather systems alternated between warm and cold on a weekly time scale from November through early January. An AR cold eastern US event between 100 and 80° W starts in early January and continues through March (Fig. 4C). Alaska and the western US was warm and the central and northeastern US was cold (Fig. S3A) with a typical amplified ridge/trough geopotential height pattern (Figs. S3B and S3C). Even though the marine Arctic near Alaska had a delayed sea ice freeze-up, the late date and short duration of the January 2014 AR pattern suggests a possible weak Arctic thermodynamic linkage.

3.6. Contrasting years

Recent Decembers in 2011 and 2016 represent years when the Northern Hemisphere circulation is more climatological/zonal with a weak ridge over the US west coast, lasting through most of the month (Fig. 7B and D). Temperature anomalies in 2011 (Fig. 7A) were slightly positive over the east coast US.

The December 2016 geopotential height field (Fig. 7D) is an example where the axis of the NA trough has shifted eastward from its climatological position into the North Atlantic south of Greenland; there are low heights over Baffin Bay in contrast to the GBB pattern. Further there is a strong zonal wind pattern across the northern North Pacific and continuing across the continent.

Other winters are dominated by progressive systems. This is shown by contrasting progressive type winters 2012–13 and 2015–16 (Fig. 4B and D) with the more stationary winters discussed earlier, 2010–11 (Fig. 4A). Progressive systems are shown as sloping contours on the Hovmoller plots. For example in 2012–13 (Fig. 4B) there are high heights beginning at New Year's day near 130° W that propagate to 60° W by mid-January. Likewise 2015–16 (Fig. 4D) has features that propagate from the Pacific (160° W) to 60° W during mid-November to mid-December, and again from mid-December to mid-January. Such rapid movement forestalls enough time for Arctic thermodynamic forcing to have much influence on the long wave pattern.

We thus show two patterns where the Arctic could reinforce existing

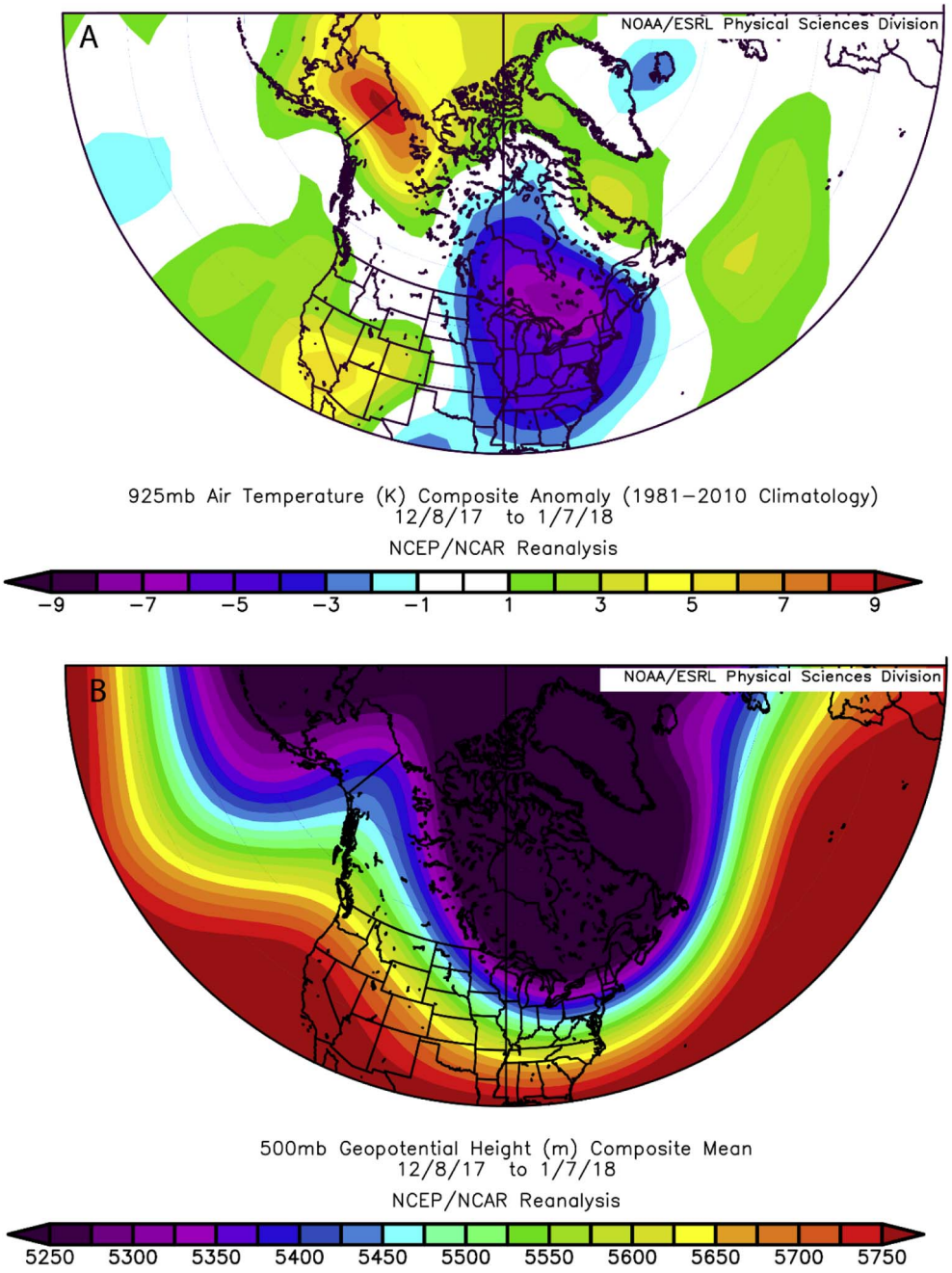

Fig. 6. Fields that represent an Alaska Ridge case from December 2017. A) 925 hPa air temperature anomaly from 8 December through 7 January 2018 shows the monthly persistence of an eastern US cold event. B) corresponding 500 hPa geopotential height field shows the strong AR pattern extending into Alaska.

jet stream wave amplitudes over NA, AR and GBB, and three examples where North American Arctic/midlatitude linkages through Arctic forcing would be weak or non-existent even if there were major regional sea ice loss: strong zonal flow, progressive weather systems, and an unfavorable orientation of the phasing of the long wave pattern. All cases are manifestations of the inherent variability of geopotential height fields and complexity of jet stream dynamics.

4. Discussion: limitations in Arctic/midlatitude weather research

There is still the need to search for emergent properties of wintertime atmospheric flow fields, constrained by hemispheric dimensions, orography, regional thermodynamic forcing, and Rossby wave scaling. Screen and Simmonds (2014) note the lack of changes in seasonal cold over the last three decades and discount Arctic impacts based on seasonal and large domain statistics. Further, Screen et al. (2015) and Ayarzagüena and Screen (2016) show future decreases in the frequency of occurrence of record breaking cold seasons. Cold linkages can occur, however, on an episodic and regional basis (Overland et al., 2015, Shepherd, 2016, and references therein), but are limited by state dependence of the jet stream orientation.

The Arctic is not the primary forcing or cause for the evolution of midlatitude weather, but increased regional Arctic geopotential thickness from delayed sea ice freeze-up can reinforce the duration of existing high amplitude waves in the geopotential height field. Analyses that average over large regions or seasonal averages will obscure rather than clarify such linkage events. Contrasting seasonal/event results can be reconciled noting that in winters that included such cold events, the overall winter may not show cooler statistics (Screen et al., 2015). Given the known intermittency in linkages, a correlation cause and

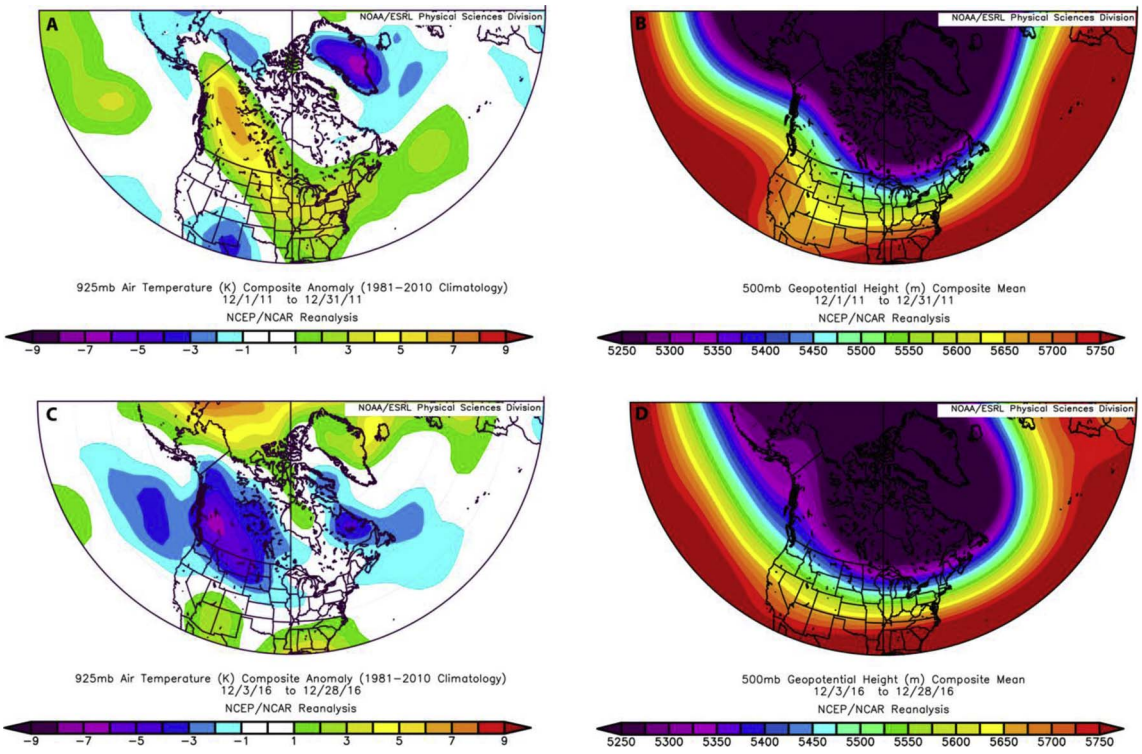

Fig. 7. A, C) Panels show 925 hPa air temperature anomalies, and B, D) show 500 hPa geopotential height fields for two Decembers with primarily zonal flow (top 2011 and bottom 2016). The height fields resemble the climatological mean fields. Figures derived from the NOAA ESRL plotting routines.

effect approach is limiting. Arctic forcing can be present, but midlatitude linkages are only apparent when proper atmospheric background flow fields exist.

The jet stream is largely characterized by non-linear interactions between enhanced atmospheric planetary waves, irregular transitions between zonal and meridional flows, maintenance of atmospheric blocks, and near stationary large amplitude atmospheric waves (Weaver, 1948; Blackmon, 1976; Dole, 1986; Masato et al., 2008; Franzke et al., 2015; Hannachi et al., 2017). These waves can be forced directly by thermodynamics or by additive and multiplicative noise (Holton, 1979; Sura et al., 2005). When the noise depends on the state of the long wave system itself, then the noise is multiplicative (Sura and Hannachi, 2015). The main trigger mechanisms for atmospheric wave structure (number of complete waves along a latitude circle), their phasing at different longitude locations, and when they propagate are not well understood, and transitions remain hard to predict.

Further, due to complexity and chaotic behavior, the linkage problem may be computationally irreducible; the only way to know the result of these interactions is to trace out their path over time through multiple ensembles. This has been shown by the large range of results from different ensemble member model solutions to ostensibly the same physical problem (Barnes and Polvani, 2015; Jaiser et al., 2016; Wu and Smith, 2016). Linkage impacts are shown in some ensemble solutions but not in others. Future model coordination activities may help (Screen, 2017) but the issue may more revolve around coming to grips with an intermittency interpretation rather than direct cause and effect hypothesis testing such as removing sea ice.

5. A problematic way forward

We point out the particularly episodic nature of both AR and GBB links to eastern US cold events and their potential linkage to Arctic surface thermodynamics. The December 2010 GBB and December 2017 AR cases are clear examples. The literature and our case study propose that physical linkage connections to delayed sea ice freeze-up are in support, but not initiation of midlatitude cold anomalies over eastern NA. Indeed there are many cold eastern NA cases that occurred in the historical record before the recent major sea ice reduction (Table 1). Also many eastern NA early winter months in the last decade did not have cold events (Table 2), and their meteorology was characterized by zonal and/or progressive geopotential height fields, despite decadal Arctic temperature amplification.

For forecast improvement in the face of computational irreducibility, a direct Numerical Weather Prediction approach is appropriate: an improved Arctic observation network feeding a data assimilation system, initializing a set of improved numerical model ensembles. Such is the plan for the ongoing Year of Polar Prediction.

Acknowledgments

We appreciate the support of the Arctic Research Program of the NOAA Climate Program Office. This is PMEL Contribution 4699. This work was partially funded by the Joint Institute for the Study of the Atmosphere and Ocean (JISAO) under NOAA Cooperative Agreement NA15OAR4320063 (2015–2020), Contribution No. 2017-099. Conflicts of interest: none. Data are routinely available from the NCAR-NCEP Reanalysis Project. Plotting routines are from the NOAA/ESRL website.

Appendix A. Supplementary data

Supplementary data related to this article can be found at http://dx.doi.org/10.1016/j.polar.2018.02.001.

References

Ayarzagüena, B., Screen, J.A., 2016. Future Arctic sea ice loss reduces severity of cold air outbreaks in midlatitudes. Geophys. Res. Lett. 43, 2801–2809. http://dx.doi.org/10.1002/2016GL068092.

Ballinger, T.J., Hanna, E., Hall, R.J., Miller, J., Ribergaard, M.H., Høyer, J.L., 2017. Greenland coastal air temperatures linked to Baffin Bay and Greenland Sea ice conditions during autumn through regional blocking patterns. Climate Dyn. http://dx.doi.org/10.1007/s00382-017-3583-3.

Barnes, E.A., Polvani, L.M., 2015. CMIP5 projections of Arctic amplification, of the North American/North Atlantic circulation, and of their relationship. J. Climate 28, 5254–5271. http://dx.doi.org/10.1175/JCLI-D-14-00589.1.
Baxter, S., Nigam, S., 2015. Key role of the north Pacific oscillation–west Pacific pattern in generating the extreme 2013/14 North American winter. J. Climate 28, 8109–8117. http://dx.doi.org/10.1175/JCLI-D-14-00726.1.
Blackmon, M.L., 1976. A climatological spectral study of the 500 mb geopotential height of the Northern Hemisphere. J. Atmos. Sci. 33, 1607–1623.
Chen, X., Luo, D., 2017. Arctic sea ice decline and continental cold anomalies: upstream and downstream effects of Greenland blocking. Geophys. Res. Lett. 44, 3411–3419. http://dx.doi.org/10.1002/2016GL072387.
Cohen, J., Screen, J.A., et al., 2014. Recent Arctic amplification and extreme mid- latitude weather. Nat. Geosci. 7, 627–637. http://dx.doi.org/10.1038/ngeo2234.
Dole, R.M., 1986. Persistent anomalies of the extra-tropical Northern Hemisphere wintertime circulation: Structure. Mon. Wea. Rev. 114, 178–207.
Francis, J.A., 2017. Why are Arctic linkages to extreme weather still up in the air? Bull. Amer. Meteor. Soc. http://dx.doi.org/10.1175/BAMS-D-17-0006.1.
Francis, J.A., Vavrus, S.J., Cohen, J., 2017. Amplified Arctic warming and mid-latitude weather: new perspectives on emerging connections. WIREs Climate Change, e474. http://dx.doi.org/10.1002/wcc.474.
Franzke, C.L.E., O'Kane, T.J., Berner, J., Williams, P.D., Lucarini, V., 2015. Stochastic climate theory and modeling. WIREs Clim. Change 6, 63–78. http://dx.doi.org/10.1002/wcc.318.
Grotjahn, R., Black, R., Leung, R., et al., 2016. North American extreme temperature events and related large scale meteorological patterns: a review of statistical methods, dynamics, modeling, and trends. Clim Dyn. 46 (1151). https://doi.org/10.1007/s00382-015-2638-6.
Hannachi, A., Straus, D.M., Franzke, C.L.E., Corti, S., Woollings, T., 2017. Low-frequency nonlinearity and regime behavior in the Northern Hemisphere extratropical atmosphere. Rev. Geophys. 55, 199–234. http://dx.doi.org/10.1002/2015RG000509.
Harnik, N., Messori, G., Caballero, R., Feldstein, S.B., 2016. The Circumglobal North American wave pattern and its relation to cold events in eastern North America. Geophys. Res. Lett. 43, 11,015–11,023. http://dx.doi.org/10.1002/2016GL070760.
Holton, J.R., 1979. An Introduction to Dynamic Meteorology, second ed. Academic Press, New York, pp. 416.
Jaiser, R., Nakamura, T., Handorf, D., Dethloff, K., Ukita, J., Yamazaki, K., 2016. Atmospheric winter response to Arctic sea ice changes in reanalysis data and model simulations. J. Geophys. Res. Atmos. 121 (13), 7564–7577. http://dx.doi.org/10.1002/2015JD024679.
Jung, T., et al., 2015. Polar-lower latitude linkages and their role in weather and climate prediction. Bull. Amer. Meteor. Soc. 96, ES197–ES200. http://dx.doi.org/10.1175/BAMS-D-15-00121.1.
Konrad, C.E.I., 1996. Relationships between the intensity of cold air outbreaks and the evolution of synoptic and planetary scale features over North America. Mon. Wea. Rev. 124, 1067–1083.
Kretschmer, M., Coumou, D., Agel, L., Barlow, M., Tziperman, E., Cohen, J., 2018. More-persistent weak stratospheric polar vortex states linked to cold extremes. Bull. Amer. Meteor. Soc. http://dx.doi.org/10.1175/BAMS-D-16-0259.1. (in press).
Kug, J.-S., Jeong, J.-H., Jang, Y.-S., Kim, B.-M., Folland, C.K., Min, S.-K., Son, S.-W., 2015. Two distinct influences of Arctic warming on cold winters over North America and East Asia. Nat. Geosci. 8, 759–762. http://dx.doi.org/10.1038/ngeo2517.
Kuhn, T.S., 2012. The Structure of Scientific Revolutions. 50th Anniversary, fourth ed. University of Chicago Press, 978-0-226-45811-3pp. 264.
Lee, M.-Y., Hong, C.-C., Hsu, H.-H., 2015. Compounding effects of warm sea surface temperature and reduced sea ice on the extreme circulation over the extratropical North Pacific and North America during the 2013–2014 boreal winter. Geophys. Res. Lett. 42, 1612–1618. http://dx.doi.org/10.1002/2014GL062956.
Liu, Z., Jian, Z., Yoshimura, K., Buenning, N.H., Poulsen, C.J., Bowen, G.J., 2015. Recent contrasting winter temperature changes over North America linked to enhanced positive Pacific-North American pattern. Geophys. Res. Lett. 42, 7750–7757. http://dx.doi.org/10.1002/2015GL065656.
Masato, G., Hoskins, B.J., Woollings, T.J., 2008. Can the frequency of blocking be described by a red noise process? J. Atmos. Sci. 66, 2143–2149.
Messori, G., Caballero, R., Gaetani, M., 2016. On cold spells in North America and storminess in western Europe. Geophys. Res. Lett. 43, 6620–6628. http://dx.doi.org/10.1002/2016GL069392.
Mills, C.M., Cassano, J.J., Cassano, E.N., 2016. Midlatitude atmospheric responses to Arctic sensible heat flux anomalies in Community Climate Model, Version 4. Geophys. Res. Lett. 43, 12,270–12,277. http://dx.doi.org/10.1002/2016GL071356.
National Research Council (NRC), 2014. Linkages between Arctic Warming and Mid-latitude Weather Patterns: Summary of a Workshop. The National Academies Press, pp. 85. Available online at: http://www.nap.edu/catalog/18727/linkages-between-arctic-warming-and-midlatitude-weather-patterns.
Ogi, M., Rysgaard, S., Barber, D., 2016. Cold winter over North America: the influence of the east Atlantic (EA) and the tropical/northern Hemisphere (TNH) teleconnection patterns. Open Atmos. Sci. J. 10, 6–13. http://dx.doi.org/10.2174/1874282301610010006.
Overland, J., Francis, J.A., Hall, R., Hanna, E., Kim, S.-J., Vihma, T., 2015. The melting Arctic and midlatitude weather patterns: are they connected? J. Climate 28, 7917–7932. http://dx.doi.org/10.1175/JCLI-D-14-00822.1.
Overland, J.E., et al., 2016. Nonlinear response of mid-latitude weather to the changing Arctic. Nat. Climate Change 6, 992–999. http://dx.doi.org/10.1038/nclimate3121.
Overland, J.E., Wang, M., 2017. Potential Arctic connections to eastern North American cold winters. Czech Polar Rep. 7 (2). http://www.sci.muni.cz/CPR/Issues14.htm.
Screen, J.A., 2017. Climate science: far-flung effects of Arctic warming. Nat. Geosci. 10, 253–254. http://dx.doi.org/10.1038/ngeo2924.
Screen, J.A., Simmonds, I., 2014. Amplified mid-latitude planetary waves favour particular regional weather extremes. Nat. Climate Change 4, 704–709. http://dx.doi.org/10.1038/nclimate2271.
Screen, J.A., Deser, C., Sun, L., 2015. Reduced risk of North American cold extremes due to continued Arctic sea ice loss. Bull. Amer. Meteor. Soc. 96, 1489–1503. http://dx.doi.org/10.1175/BAMS-D-14-00185.1.
Shepherd, T.G., 2016. Effects of Arctic warming. Science 353, 989–990. http://dx.doi.org/10.1126/science.aag2349.
Singh, D., Swain, D.L., Mankin, J.S., Horton, D.E., Thomas, L.N., Rajaratnam, B., Diffenbaugh, N.S., 2016. Recent amplification of the North American winter temperature dipole. J. Geophys. Res. Atmos. 121, 9911–9928. http://dx.doi.org/10.1002/2016JD025116.
Sura, P., Hannachi, A., 2015. Perspectives of non-Gaussianity in atmospheric synoptic and low-frequency variability. J. Clim. 28, 5091–5114.
Sura, P., Newman, M., Penland, C., Sardeshmukh, P., 2005. Multiplicative noise and non-Gaussianity: a paradigm for atmospheric regimes? J. Atmos. Sci. 62, 1391–1409.
Wallace, J.M., Held, I.M., Thompson, D.W.J., Trenberth, K.E., Walsh, J.E., 2014. Global warming and winter weather. Science 343, 729–730. http://dx.doi.org/10.1126/science.343.6172.729.
Weaver, W., 1948. Science and complexity. Amer. Sci. 36, 536–544.
Wu, Y., Smith, K.L., 2016. Response of Northern Hemisphere midlatitude circulation to Arctic amplification in a simple atmospheric general circulation model. J. Climate 29, 2041–2058. http://dx.doi.org/10.1175/JCLI-D-15-0602.1.
Xie, Z., Black, R.X., Deng, Y., 2017. The structure and large-scale organization of extreme cold waves over the conterminous United States. Climate Dyn. http://dx.doi.org/10.1007/s00382-017-3564-6.